EEG-Based Brain-Computer Interfaces Using Gazelle Optimization Algorithm with Deep Learning for Motor-Imagery Classification

P. Radhakrishnan[1], Abullaıs Nehal Ahmed[2], K. Kalaiarasi[3,*], Koppisetti Giridhar[4], S. Thenappan[5]

[1]Department of ECE, Tagore Engineering College, Rathinamangalam, Kelambakkam - Vandalur Rd, Chennai, 600127, India
[2]J.A.T. Arts, Science and Commerce College (for Women), Malegaon, Dist. Nashik, Maharashtra, India
[3]Department of ECE, Saveetha School of Engineering, Saveetha Institute of Medical and Technical Sciences, Chennai, India
[4]Department of Computer Science & Technology, Madanapalle Institute of Technology & Science, Madanapalle, Andhra Pradesh, India
[5]Department of Electronics and Communication Engineering, Vel Tech Rangarajan Dr. Sagunthala R&D Institute of Science and Technology, Chennai, India.
Emails: krish75radha@gmail.com; aabullais@gmail.com; kalaiarasik.sse@saveetha.com; kgiridhar562@gmail.com; drthenappans@veltech.edu.in

Abstract

Brain-computer interface (BCI) is a procedure of connecting the central nervous system to the device. In the past few years, BCI was conducted by Electroencephalography (EEG). By linking EEG with other neuro imaging technologies like functional Near Infrared Spectroscopy (fNIRS), promising outcomes were attained. An important stage of BCI is brain state identification from verified signal properties. Classifying EEG signals for motor imagery (MI) is a common use in the BCI system. Motor imagery includes imagining the movement of certain body parts without executing the physical movement. Deep Artificial Neural Network (DNN) obtained unprecedented complex classification outcomes. Such performances were obtained by an effective learning algorithm, improved computation power, restricted or back-fed neuron connection, and valuable activation function. Therefore, this study develops a Gazelle Optimization Algorithm with Deep Learning based Motor-Imagery Classification (GOADL-MIC) technique for EEG-Based BCI. The GOADL-MIC technique aims to exploit hyperparameter-tuned DL model for the recognition and identification of MI signals. To achieve this, the GOADL-MIC model initially undergoes the conversion of one dimensional-EEG signals into 2D time-frequency amplitude one. Besides, the EfficientNet-B3 system is applied for the effectual derivation of feature vector and its hyperparameters can be selected by using GOA. Finally, the classification of MIs takes place using bi-directional long short-term memory (Bi-LSTM). The experimentation result analysis of the GOADL-MIC method is verified utilizing the BCI dataset and the results demonstrate the promising results of the GOADL-MIC algorithm over its counter techniques

Keywords: Brain-computer interfaces; EEG signals; Deep learning; Motor imagery signals; Image classification

1. Introduction

A Brain-Interface Computer (BCI) is an emerging technology which allows direct communication amongst a computer and the human brain. BCI is majorly employed as a technology for utilizing the electrical activity in the brain to diagnose neurological diseases, in disabled patients who have lost their capabilities and to comprehend psycho-physiological processes [1]. Electroencephalography (EEG) is a non-invasive BCI system wherein brain actions have been taken with a higher temporal resolution, usability, portability and lower setup cost [2]. In applications that include handicapped patients, BCI is often implemented as a system to restore those fundamental abilities by making data pathways among the processing or computing devices and the human brain [3].

Doi: https://doi.org/10.54216/FPA.160103
Received: July 24, 2023 Revised: November 27, 2023 Accepted: April 18, 2024

Alternatively stated, a BCI technique employs the information from the brain activity in physically handicapped persons to support them when mapping their sensory-motor functions. EEG equipment has been extensively employed for recording brain signals in BCI systems due to it being non-invasive, higher time resolution, possible for mobility in the user and a moderately lower cost [4]. While a BCI must be developed to utilize EEG signals in a wide range of methods for controlling motor imagery (MI) BCIs, are liable to wide-ranging research. This is due to their expansive capabilities for applicability in domains namely neuroprosthetics, neurorehabilitation, and gaming, where the decoding of users' opinions of an imagined activity will be inestimable [5].

MI is the most widespread technique in BCI applications that includes performing a motor task only by imagining or thinking. This will be just an easy moving of legs or hands and closing eyes [6]. Therefore, MI-based BCI techniques become a noticeable solution for identifying the preferred commands by categorizing MI tasks for disabled persons of their motor capacities and rehabilitation. However, MI signals can be extremely non-stationary and unavoidably affected by noise while they are intensely dependent upon subjects. Furthermore, the classification of EEG can be generally a difficult and aperiodic time series that is the addition of a huge number of neuronal membrane possibilities [7]. Hence, a robust pattern identification system could be essential for the execution of an MI-based BCI system with a higher performance. The machine learning (ML) method has been frequently employed in this classification method as it can be the capability to model higher-dimensional datasets [8]. ML technique could be briefly described as allowing computers to create effective predictions with the help of previous knowledge. In ML, there are numerous approaches for classification methods namely Logistic Regression (LR), Decision Tree (DT), Naïve Bayes (NB), K-Nearest Neighbors (KNN), and Support Vector Machine (SVM). Deep learning (DL) algorithms are great at developing the higher dimensional feature space as well as decreasing the lesser dimension. It is promising to include each potential EEG channel in this research, with high-frequency bandwidth without feature selection (FS), which is barely implemented in prior BCI research [9, 10].

This study develops a Gazelle Optimization Algorithm with Deep Learning based Motor-Imagery Classification (GOADL-MIC) technique for EEG-Based BCI. The GOADL-MIC technique aims to exploit hyperparameter-tuned DL model for the recognition and identification of MI signals. To achieve this, the GOADL-MIC system initially undergoes the conversion of one dimensional-EEG signals into 2D time-frequency amplitude one. Besides, the EfficientNet-B3 system can be applied for the effectual derivation of feature vector and its hyperparameters can be chosen by the use of GOA. Finally, the classification of MIs takes place using bidirectional long short-term memory (Bi-LSTM). The experimental result study of the GOADL-MIC system is tested using the BCI dataset.

2. Related Works

Rajalakshmi et al. [11] introduced an Optimal DL-Based Recognition for EEG Signal Motor Image (ODLR-EEGSM) models. The pre-processing stage begins with the Variation Mode Decomposition (VMD) system. This method employs a Stacked Sparse Auto Encoder (SSAE) algorithm for recognizing major patterns. This classification was accomplished by implementing the Deep Wavelet Neural Networks (DWNN) improved with the Chaotic Dragonfly Algorithm (CDFA) method. In [12], an innovative convolutional neural network (CNN) was developed. The developed EEG-inception architecture was dependent upon the backbone of the inception-time network that must be exhibited to be extremely effective for classifying time series. Similarly, the designed network becomes an end-wise classification, as it captures the raw input signal and doesn't need pre-processing of complex EEG signals. Additionally, this study offers a new data augmentation technique for increasing the accuracy of EEG signals. Wang, Yang, and Huang [13] proposed an unsupervised DTL-based system. The Euclidean space data alignment (EA) technique could be employed for aligning the target field EEG information. Afterward, the common spatial pattern (CSP) has been utilized for extracting feature, and the DCNN was implemented to classify EEG.

In [14], a deep domain adaptation framework with a correlation alignment (DDAF-CORAL) method was designed. Particularly, a 2 phase architecture was employed for extracting deep features for original EEG information. The allocation difference provided by context-relevant and time-relevant differences was also minimalized by aligning the target EEG feature distributions and covariance of the source. Lastly, the classification and adaptation losses have been enhanced concurrently to attain satisfactory discriminative classification effectiveness and lower feature distribution divergence. Cho, Jeong, and Lee [15] projected NeuroGrasp, a dual-phase DL technique that interprets numerous hand clutching from EEG signals in the MI model. This presented technique efficiently utilizes an EEG and EMG-based learning, this EEG-based inference in the test stage will be achievable. The EMG control in model training enables BCIs to precisely forecast hand grasp categories from EEG signals. In [16], a pre-processing method was presented for the representation of EEG signals. Next, a parallel-CNN (PCNN) model was designed

Doi: https://doi.org/10.54216/FPA.160103
Received: July 24, 2023 Revised: November 27, 2023 Accepted: April 18, 2024

for categorizing motor imagery signals. Innovative types of images were produced to integrate spatial filtering and frequency band extractor for the depiction of raw EEG signals. With the help of providing the signified images into the PCNN, it loads combination of a 3 unique sub-methods targeting for increasing the effectiveness of classification.

Liu et al. [17] introduced an innovative end wise system to decode MI-EEG signal, dense multi-branch 1D-CNN (CMO-CNN), without any pre-processing namely filtering, employing the EEG signals. The one dimensional convolutional was exploited as a feature extraction for extracting various and multi-class feature in fusion through diverse filter scales and depths of various types. 1D SE-block and alternative links have been included to enhance the generalization and powerful network. The authors [18] provided an end-wise DL model, named EEG channel active inference-NN (EEG-ARNN) that was dependent upon graph CNNs (GCN) to completely use the connection of signals in the domain of temporal and spatial. Two channel selection algorithms, such as aggregation-selection (AS) and edge-selection (ES), have been developed for automatically choosing a particular number of optimum channels.

3. The Proposed Model

In this work, the automatic GOADL-MIC technique was introduced for the recognition and identification of EEG signals for the MI classification procedure. The GOADL-MIC technique comprises several processes such as pre-processing, EfficientNet-B3-based feature extraction, BiLSTM-based classification and GOA-based hyperparameter tuning. Fig. 1 illustrates the workflow of GOADL-MIC system.

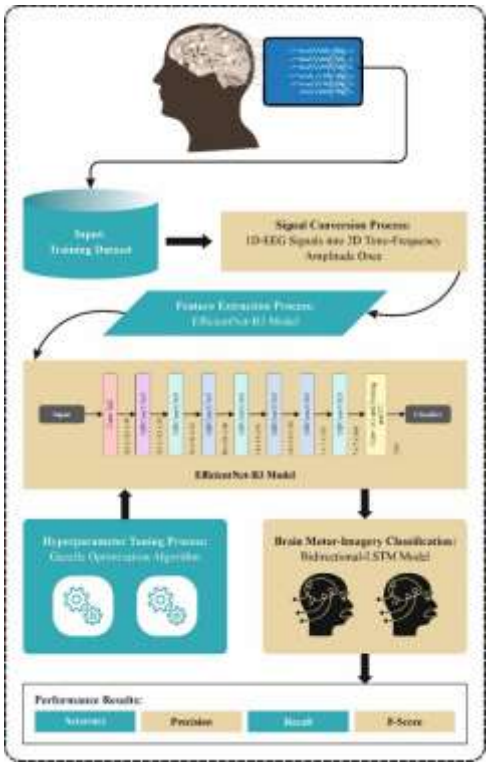

Figure 1: Workflow of GOADL-MIC technique

A. Pre-processing

In this work, the initial phase of pre-processing is performed via the CWT method. CWT is a widely used approach to change a one-dimensional signal into two-dimensional matrix in the frequency domain [19]. The WT is nothing but an effective model, the time-frequency alter than the standard cosine and Fourier transform (FT). The FT which produces a spectrogram with secure resolution of time-frequency, WT combines varying rules and for that reason, it offers optimal resolution of time-frequency. The wavelet filtering bank makes use of logical Morse wavelet with time-bandwidth creation and symmetry parameter equal to 60 and 3, respectively. In the meantime, the image of scalogram WT is denoted by 69x400, rescaled to 224x224 over bicubic interpolation.

B. Feature Extraction using EfficientNet-B3 Model

Doi: https://doi.org/10.54216/FPA.160103
Received: July 24, 2023 Revised: November 27, 2023 Accepted: April 18, 2024

In the GOADL-MIC technique, the EfficientNet-B3 model can be employed. When EfficientNet CNN techniques were employed in the dataset of ImageNet, they established that their methods outpaced the entire current methods concerning the amount of top 1 parameters and accuracy. A new technique to scale CNN technique is the basis for the EfficientNet model. It creates usage of a direct and great compound co-efficient. Exclusively in comparison to conventional plans that scale features like width, wisdom, and objective. EfficientNet measures every feature with an appropriate set of scaling co-efficient reliably. Scaling individual features functions on model implementation but altering all modules about the available assets functions on complete implementation [20].

When compared to other models, EfficientNet is much lesser with ImageNet accuracy equivalent to its individual. For example, the ResNet_50 technique has 23,534,592 limitations. It is required to meet the prospects of the smallest Efficient Net (named EfficientNet_B0), which consumes 5,330,564 limits. We presented an effectual technique depending upon the Efficient Net_B3 CNN technique because it attacks good stability among accuracy as well as computational power. The main factor of the EfficientNet method is MBConv (mobile inverted bottleneck convolution). The MobileNet methods ideas were the basis for MBConv. One of the main ideas to employ is depth-wise separable Conv, which involves a point-wise and a depth-wise Conv. The following dual extra ideas were reserved from MobileNetV2 and the second enhanced form of MobileNet such as linear bottlenecks and residual connections [20]. The EfficientNet method family starts with its stem. The stem is general to every 8 techniques and the last layers. There are 7 blocks after the stem. The complete amount of layers in EfficientNetB0 is 237, whereas the complete amount in EfficientNetB7 is 813. The 2nd element is the basis for the 1st sub-block of the 7 major blocks, excluding the first. Module 3 is linked to the sub-block through the skip connection. In the first sub-blocks, the skip connection has been integrated with Module 4. Module 5 transports collectively every sub-block by linking it in a skip way to the one beforehand. Lastly, subblocks are generated by uniting the modules being employed in the exact method in the block.

C. Hyperparameter Tuning using GOA

The GOADL-MIC technique employs the GOA for the hyperparameter tuning process. GOA is based on the existence capabilities of gazelles which leverage the gazelles' adaptive features for real-time optimizer issues. This model incorporates the lower bound (LB) and upper bound (UB) constraints for establishing the allowable range of value for the population and also, and its technique exploits gazelles as searching agents that are denoted by $n \times d$ [21].

$$X = \begin{bmatrix} x_{1,1} & x_{1,2} & \cdots & x_{1,d-1} & x_{1,d} \\ x_{2,1} & x_{2,2} & \cdots & x_{2,d-1} & x_{2,d} \\ \vdots & \vdots & x_{i,j} & \vdots & \vdots \\ x_{n,1} & x_{n,2} & \cdots & x_{n,d-1} & x_{n,d} \end{bmatrix} \tag{1}$$

Where the candidate population (position vector matrix) is represented as X. LB_j and UB_j are the lower and upper boundaries, correspondingly, $rand$ refers to the random values. n and d variables are the gazelle and the dimensionality, correspondingly.

$$x_{i,j} = rand \times \left(UB_j - LB_j\right) + LB_j \tag{2}$$

After producing candidate solutions by $x_{i,j}$ in all the iterations, the potential solution is recognized as the minimum solution. The best gazelles establish extraordinary skills in predator evasion, threat recognition, and warning others, the fittest gazelles are designated as the optimum solution obtained so far. Eq. (3) is used to create the Elite $n \times d$ matrix, which acts as a reference to guide the gazelle in defining the subsequent step during the search stage.

$$Elite = \begin{bmatrix} x'_{1,1} & x'_{1,2} & \cdots & x'_{1,d-1} & x'_{1,d} \\ x'_{2,1} & x'_{2,2} & \cdots & x'_{2,d-1} & x'_{2,d} \\ \vdots & \vdots & x'_{i,j} & \vdots & \vdots \\ x_{n,1} & x_{n,2} & \cdots & x_{n,d-1} & x_{n,d} \end{bmatrix} \tag{3}$$

Where $x'_{i,j}$ denotes the location vector of the leading gazelle. After each iteration, the Elite matrix is dynamically updated when the better gazelle exceeds the present top gazelles. We apply a controlled Brownian movement represented by the regulated and uniform step to safeguard effective search of neighboring areas. This stochastic movement is subjected to the Gaussian (likelihood distribution) function, with variance (σ^2) 1 and mean (μ) 0. The Brownian movement can be described using Eq. (4),

$$f_B(x, \mu, \sigma) = \frac{1}{\sqrt{2\pi\sigma^2}} e\left(-\frac{(x-\mu)^2}{2\sigma^2}\right) = \frac{1}{\sqrt{2\pi}} e\left(-\frac{x^2}{2}\right) \tag{4}$$

Doi: https://doi.org/10.54216/FPA.160103
Received: July 24, 2023 Revised: November 27, 2023 Accepted: April 18, 2024

At the time of grazing, a Brownian movement pattern is modeled for the gazelle's movement. This can be mathematically modeled as follows:

$$g_{i+1} = g_i + s \cdot R *\cdot R_B *\cdot (Elite_i - R_B *\cdot g_i) \quad (5)$$

Whereg_i and g_{i+1} are the solutions attained in the existing and subsequent iterations. The parameter "s" shows the grazing velocity of the gazelle. The vector R_B is a random number that simulates Brownian movement, and R is a uniformly distributed random number within [0,1]. Once the predator is discovered, the exploration stage begins. In this phase, the Lévy fight strategy is adopted, integrating occasional long jumps and short steps. The mathematical expression of Lévy is given below [21]:

$$L(x_j) \approx |x_j|^{1-\alpha} \quad (6)$$

Where the fight distance is represented as x_j, and the power-law exponent is α in [1, 2]:

$$f_L(x;\alpha,\gamma) = \frac{1}{\pi}\int_0^{\infty} exp(-\gamma q^{\alpha})cos(qx)\delta q \quad (7)$$

In Eq. (7), the movement is controlled by the distribution index (α), and γ denotes the scaling unit. GOA produces stable Lévy movement by accepting $the\ \alpha$ value, and its formula is given below.

$$Levy(\alpha) = 0.05 \times \frac{x}{|y|^{\frac{1}{\alpha}}} \quad (8)$$

Where y and x are a uniform distribution with variance 1 and mean 0.

$$\sigma_x = \left(\frac{\mathrm{r}(1+\alpha)\sin\left(\frac{\pi\alpha}{2}\right)}{\mathrm{r}\left(\frac{1+\alpha}{2}\right)\alpha 2^{\left(\frac{\alpha-1}{2}\right)}}\right)^{1/\alpha} \quad (9)$$

In optimization studies, this algorithm has shown improved search capability. The gazelle applies LF for its escape. The gazelle behaviors in finding predators can be mathematically described as follows:

$$\overrightarrow{g_{\iota+1}} = \overrightarrow{g_\iota} + S \cdot \mu \cdot \vec{R} *\cdot \overrightarrow{R_L} *\cdot \left(\overrightarrow{Elite_\iota} - \overrightarrow{R_L} *\cdot \overrightarrow{g_\iota}\right) \quad (10)$$

In Eq. (10), S denotes the top speed that the gazelles could achieve, $\overrightarrow{and\ R_L}$ shows the Lévy distribution-based random vector. The predator chases the gazelle can be expressed by,

$$\overrightarrow{g_{\iota+1}} = \overrightarrow{g_\iota} + S \cdot \mu \cdot CF *\cdot \overrightarrow{R_B} *\cdot (\overrightarrow{Elite_\iota} - \overrightarrow{R_B} *\cdot \overrightarrow{g_\iota}) \quad (11)$$

Where CF denotes the cumulative effects of the predator, evaluated as $CF = (1 - iter/iterMax)$. The PSR (predator success rate) affects the gazelle's capability to prevent local minima. $\vec{U}$ refers to the binary vector produced by random value r within [0,1] so that $\vec{U} = 0$ for $r < 0.34$; or else $\vec{U} = 1$.

$$\overrightarrow{g_{\iota+1}} = \begin{cases} \overrightarrow{g_\iota} + CF\left[\overrightarrow{LB} + \vec{R} *\cdot \left(\overrightarrow{UB} - \overrightarrow{LB}\right)\right] *\cdot \vec{U}; \\ if\ r \le PSRs \\ \overrightarrow{g_\iota} + [PSRs(1-r) + r](\overrightarrow{g_{r1}} - \overrightarrow{g_{r2}}); else \end{cases} \quad (12)$$

The GOA method originates an FF to get high efficiency of classifier. It states an optimistic number to represent the finest outcome of the candidate solution. In this study, the decrease of classifier rate of error is regarded as FF that expressed below:

$$fitness(x_i) = ClassifierErrorRate(x_i)$$
$$= \frac{No.of\ misclassified\ samples}{Total\ No.of\ samples} * 100 \quad (13)$$

D. Image Classification using Bi-LSTM Model

For MI classification, the GOADL-MIC technique uses the Bi-LSTM model. LSTM has been designed to overcome the RNN vanishing gradient issue. In order to achieve this, the LSTM's model has been developed with

Doi: https://doi.org/10.54216/FPA.160103
Received: July 24, 2023 Revised: November 27, 2023 Accepted: April 18, 2024

3 gates like output, forget, and input [22]. The LSTM cell includes input gate i_t, output gate 0_t, and forget gate f_t which can be determined by following measures. The forget gate (f_t) can be accountable to determine whether data from the earlier state (C_{t-1}) is to be forgotten or retained. These outcomes are accomplished depending on the inputs from both the existing input vector (x_{new_r}) and the hidden layer (HL) (h_{t-1}), where the next mathematical formula can be applied to determine it:

$$f_t = \sigma\left(W_f\left[h_{t-1}, x_{new_t}\right] + b_f\right) \tag{14}$$

The Weight matrix and bias terms were described by W_f and b_f, correspondingly. Similarly, the input gate (i_t) defines how much data (x_t) and (h_{t-1}) should be accepted to upgrade the cell state, and could be determined as:

$$i_t = \sigma\left(W_i\left[h_{t-1}, x_{new_t}\right] + b_i\right) \tag{15}$$

$$\tilde{C}_{\mathrm{t}} = \tanh\left(W_c[h_{t-1)} x_{new_f}] + b_c\right) \tag{16}$$

$\tilde{C}_{\mathrm{t}}$ refers to an existing condition. To decide which data to forget and which data to reserve, the updated cell state can be given below:

$$C_t = f_t \odot C_{t-1} \odot i_t \odot \tilde{C}_{\mathrm{t}} \tag{17}$$

where the sign $\odot$ describes element-wise vector multiplication, and C_t portrays the long-term state. The data flow among the existing cell state and its HL must be measured via an output gate o_t:

$o_t = \sigma\left(W_o\left[h_{t-1}, x_{new_t}\right] + b_{\mathrm{o}}\right)$, and (18)

$$h_t = \mathrm{o}_t \odot \tanh(C_t) \tag{19}$$

Where h refers to the output. Some of the various LSTM models that could be employed such as stacked LSTM, Bi-LSTM, encoder-decoder LSTM, CNN-LSTM, and Vanilla LSTM.

Graves and Schmidhuber in 2005 proposed BiLSTM based on the BRNN with LSTM cell. It is popular in which the successive data retain higher temporal dependency. Consequently, it can be essential for evaluating the conditions in the prospect. The BiLSTM is a vital tool to handle such a condition. It consists of the fully connected (FC) layer, BiLSTM layer, and input layer. Besides, a softmax layer must be employed for the output. In these guidelines, Bi-LSTM could absorb the input to be transferred backward and forward. The forward LSTM involves data from the right to left, representing its HL in such a way: $\vec{h} = LSTM\left(x_{new}, \vec{h}_{t-1}\right)$ while the backward LSTM deals with data in the backward way and its HL should be offered $h_t = LSTM\left(x_{new}, \overleftarrow{h}_{t-1}\right)$. The structure of the Bi-LSTM system was displayed in Fig. 2.

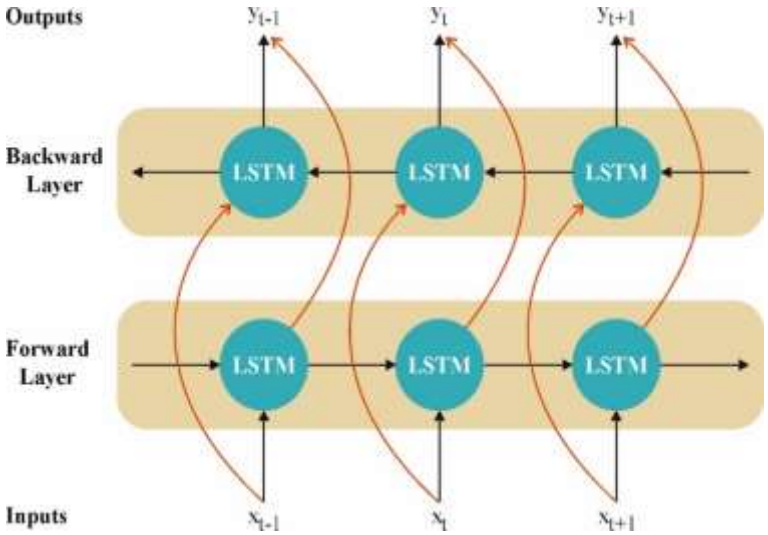

Figure 2: Architecture of Bi-LSTM model

Finally, the forward and backward conditions can be combined to produce a Bi-LSTM output in accordance with the given formula:

Doi: https://doi.org/10.54216/FPA.160103
Received: July 24, 2023 Revised: November 27, 2023 Accepted: April 18, 2024

$$h_t = [\vec{h}_t, \overleftarrow{h}_t] \tag{20}$$

Determine that the h_t last HL encodes the majority of the input features of the signal that can be further utilized as input for an FC layer targeted for converting to vector with distance according to its class count. With respect to error classification, a layer of softmax was permitted. The distribution probability can be represented as given:

$$\tilde{Y} = softmax(W_s h_f + b_s) \tag{21}$$

where b_s and W_s specify the bias and weight correspondingly.

$$softmax(z_i) = \frac{\exp(z_i)}{\sum_{j=1}^{k} \exp(z_j)} \tag{22}$$

where z_i represents the i^{th} component of the input vector z. With the help of reducing the error among actual Y and predicted $\tilde{Y}$, the Bi-LSTM architecture has been trained.

4. Results and Discussion

The experimental outcomes of the GOADL-MIC system can be examined on 2 datasets comprising BCI Competition 2003 dataset-III and BCI competition-IV dataset 2b. The BCI competition 2003, dataset-III [23], encompasses 3-channel EEG data in normal females, for the imagination of left, and right-hand activities. The BCI competition-IV dataset 2b includes 9 subjects each with 5 sessions of MI empirically, between that the main 2 sessions can be affirmed without response and the residual 3 sessions can be incorporated online feedback [24]. These datasets can be accessed by mailing the principal author of the study.

Table 1 and Fig. 3 represent the overall performance of the GOADL-MIC technique on the BCI Competition-III dataset. The accomplished findings indicate the proficient outcomes of the GOADL-MIC model below all epochs. According to 500 epochs, the GOADL-MIC technique offers $prec_n$ of 98.76%, $reca_l$ of 97.44%, $accu_y$ of 98.17%, and F_{score} of 98.29%. Meanwhile, based on 1000 epochs, the GOADL-MIC system gives $prec_n$ of 98.92%, $reca_l$ of 97.63%, $accu_y$ of 98.21%, and F_{score} of 98.27%. Moreover, with 2000 epochs, the GOADL-MIC system gives $prec_n$ of 94.93%, $reca_l$ of 98.83%, $accu_y$ of 98.93%, and F_{score} of 96.97%. Finally, based on 2500 epochs, the GOADL-MIC method gains $prec_n$ of 96.15%, $reca_l$ of 97.64%, $accu_y$ of 96.78%, and F_{score} of 96.72%, respectively.

Table 1: Overall performance of the GOADL-MIC model under the BCI Competition-III dataset

BCI Competition-III Dataset				
No. of Epoch	$\boldsymbol{Prec_n}$	$\boldsymbol{Reca_l}$	$\boldsymbol{Accu_y}$	$\boldsymbol{F_{score}}$
500	98.76	97.44	98.17	98.29
1000	98.92	97.63	98.21	98.27
1500	98.98	99.44	99.81	99.77
2000	94.93	98.83	98.93	96.97
2500	96.15	97.64	96.78	96.72
Average	97.55	98.19	98.38	98.00

Doi: https://doi.org/10.54216/FPA.160103
Received: July 24, 2023 Revised: November 27, 2023 Accepted: April 18, 2024

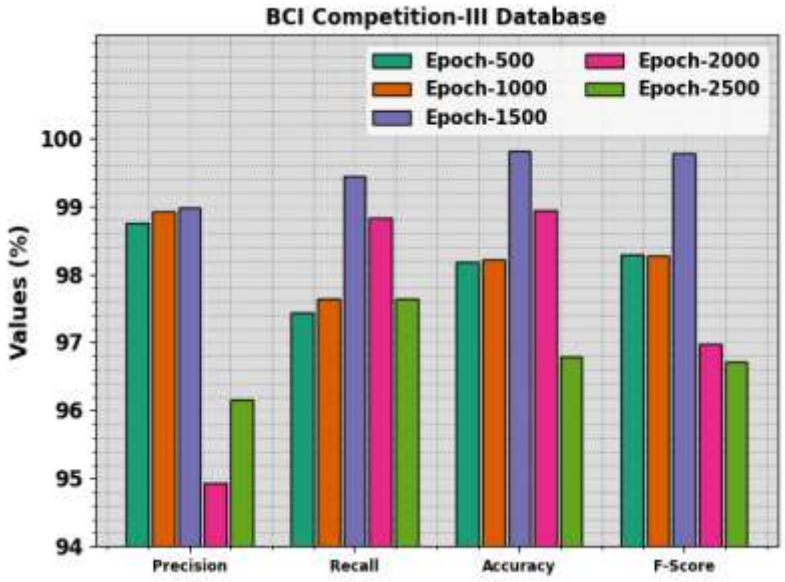

Figure 3: Overall performance of the GOADL-MIC system on the BCI Competition-III dataset

Table 2 and Fig. 4 highlight the comparative outcomes of the GOADL-MIC technique on the BCI Competition-III dataset [25]. The achieved results represent that the Improved GA FKNN-LDA system and WTSE-SVM algorithm get worse performance with least $accu_y$ values of 84.00% and 86.40%. Additionally, the Adaptive PP-Bayesian and STFT-DT models exhibit closer $accu_y$ values of 90.00% and 90.00%. Although the CWTFB-TL and AORNDL-MIC techniques offer reasonable performance, the GOADL-MIC technique highlighted a maximum $accu_y$ of 96.38%.

Table 2: $Accu_y$ analysis of the GOADL-MIC system compared with other models under the BCI Competition-III dataset

BCI Competition-III Dataset	
Models	Accuracy
Adaptive PP-Bayesian	90.00
STFT-DL Algorithm	90.00
Optimized GA FKNN-LDA	84.00
WTSE-SVM Model	86.40
CWTFB-TL Model	95.71
AORNDL-MIC Algorithm	96.14
GOADL-MIC	98.38

Doi: https://doi.org/10.54216/FPA.160103
Received: July 24, 2023 Revised: November 27, 2023 Accepted: April 18, 2024

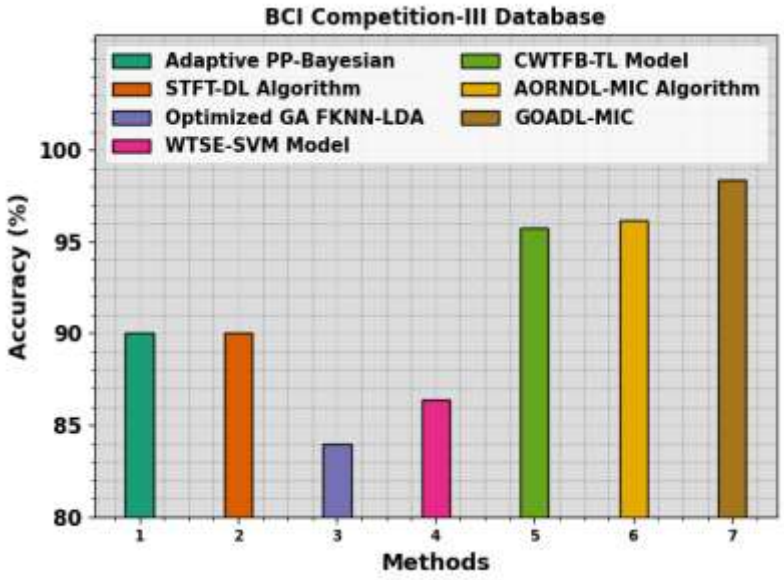

Figure 4: $Accu_y$ analysis of the GOADL-MIC technique compared with other systems

The $accu_y$ curves for training (TRA) and validation (VAL) shown in Fig. 5 for the GOADL-MIC model on the BCI Competition-III dataset provide valued insights into its effectiveness in varied epochs. Mainly, it is consistent upgrade in both TRA and TES $accu_y$ with amplified epochs, representing the ability of the system in learning and recognizing patterns from both data of TRA and TES. The higher tendency in TES $accu_y$ emphasizes the model's adaptability to the TRA dataset as well as the ability to create correct forecasts on unnoticed data, underscoring skills of strong generalization.

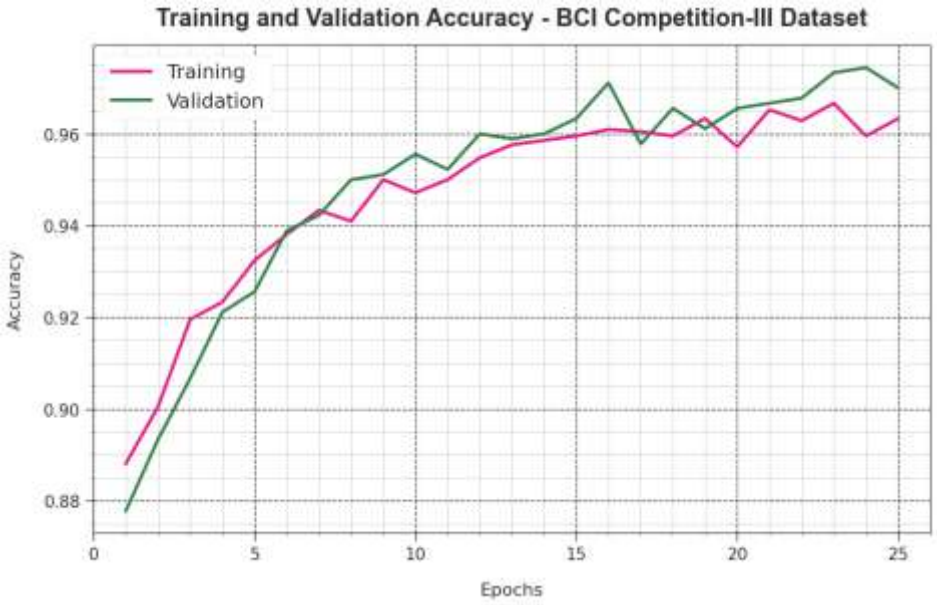

Figure 5: $Accu_y$ curve of the GOADL-MIC system with the BCI Competition-III dataset

Doi: https://doi.org/10.54216/FPA.160103
Received: July 24, 2023 Revised: November 27, 2023 Accepted: April 18, 2024

Figure 6: Loss curve of the GOADL-MIC model with the BCI Competition-III dataset

Fig. 6 establishes an extensive summary of the TRA and TES loss values for the GOADL-MIC algorithm below the BCI Competition-III dataset through numerous epochs. The TRA loss constantly reduces as the method refines weights to minimalize classifier errors under both datasets. The loss curves exhibit the model's position with the TRA data, highlighting its skill to take patterns efficiently. Noteworthy is the nonstop refinement of parameters in the GOADL-MIC model, directed at lessening discrepancies amongst predictions and real TRA labels.

The overall performance of the GOADL-MIC system under the BCI-Competition-IV dataset is reported in Table 3 and Fig. 7. The simulation results identified the proficient performance of the GOADL-MIC technique under all epochs. With S1, the GOADL-MIC technique offers $accu_y$ of 88.94%, 73.01%, 86.06%, 83.99%, and 89.96% under epochs 500-2500 respectively. Also, based on S3, the GOADL-MIC methodology provides $accu_y$ of 89.88%, 82.03%, 95.85%, 76.96%, and 87.85% on epochs 500-2500. Besides, with S5, the GOADL-MIC algorithm achieves $accu_y$ of 85.92%, 86.84%, 90.06%, 92.82%, and 83.06% on epochs 500-2500. Meanwhile, with S7, the GOADL-MIC technique gets $accu_y$ of 84.84%, 92.98%, 86.96%, 82.95%, and 96.94% on epochs 500-2500, correspondingly.

Table 3: Overall performance of the GOADL-MIC system under the BCI Competition-IV dataset

BCI Competition-IV Dataset										
No. of Epoch	S1	S2	S3	S4	S5	S6	S7	S8	S9	Average
500	88.94	86.85	89.88	88.04	85.92	77.90	84.84	97.98	84.83	87.24
1000	73.01	85.08	82.03	95.98	86.84	80.83	92.98	85.12	94.09	86.22
1500	86.06	98.09	95.85	99.88	90.06	91.94	86.96	90.93	88.88	92.07
2000	83.99	92.85	76.96	90.87	92.82	94.02	82.95	89.92	96.94	89.04
2500	83.96	82.92	87.85	93.13	83.06	88.88	96.94	91.03	83.09	87.87
Average	83.19	89.16	86.51	93.58	87.74	86.71	88.93	91.00	89.57	88.49

Doi: https://doi.org/10.54216/FPA.160103
Received: July 24, 2023 Revised: November 27, 2023 Accepted: April 18, 2024

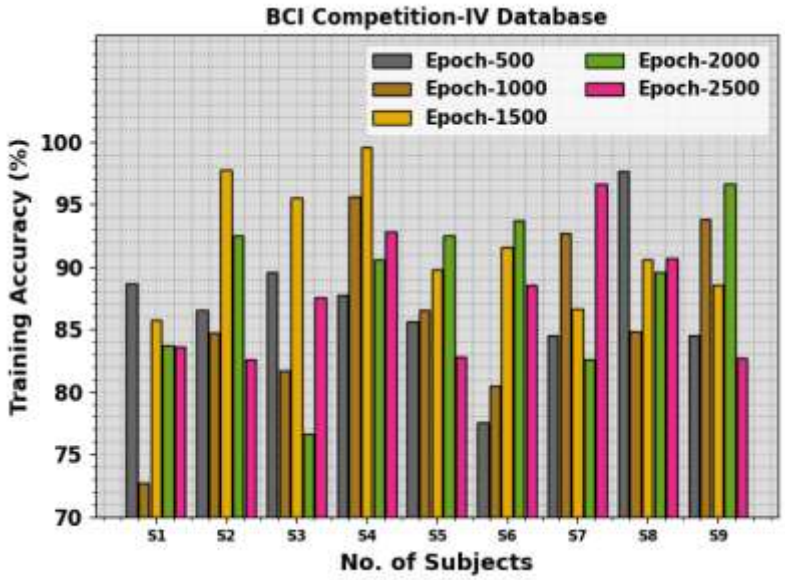

Figure 7: Overall performance of the GOADL-MIC model on the BCI Competition-IV dataset

Table 4 and Fig. 8 represent a detailed comparative analysis of the GOADL-MIC method on the BCI Competition-IV dataset [25]. These results stated that the GOADL-MIC technique reaches improved performance with each subject. According to S-1, the GOADL-MIC system gains an increased $accu_y$ of 91.90% whereas the CSP, FBCSP, FDBN, and AORNDL-MIC methodologies obtain decreased $accu_y$ values of 68.97%, 72.89%, 84.06%, and 84.14% correspondingly. Followed by, S-3, the GOADL-MIC method achieves raised $accu_y$ of 89.20% whereas the CSP, FBCSP, FDBN, and AORNDL-MIC algorithms get reduced $accu_y$ values of 59.98%, 64.17%, 69.11%, and 87.82%. Additionally, based on S-5, the GOADL-MIC method attains an increased $accu_y$ of 90.62% but the CSP, FBCSP, FDBN, and AORNDL-MIC systems get diminished $accu_y$ values of 79.78%, 96.06%, 95.99%, and 88.66%. Finally, on S-9, the GOADL-MIC method accomplishes better $accu_y$ of 92.01% however, the CSP, FBCSP, FDBN, and AORNDL-MIC systems get diminished $accu_y$ values of 86.16%, 90.04%, 93.98%, and 90.50%, respectively.

Table 4: Comparison analysis of the GOADL-MIC system under the BCI Competition-IV dataset

BCI Competition-IV Dataset					
Subject	CSP Model	FBCSP MIRSR	FDBN Model	AORNDL-MIC	GOADL-MIC
S-1	68.97	72.89	84.06	84.14	91.90
S-2	64.71	64.03	68.06	90.08	91.48
S-3	59.98	64.17	69.11	87.82	89.20
S-4	99.70	99.95	99.96	94.76	96.38
S-5	79.78	96.06	95.99	88.66	90.62
S-6	78.00	83.84	90.94	88.07	89.59
S-7	79.71	80.93	84.85	90.22	91.93
S-8	95.85	95.82	97.12	92.11	93.76
S-9	86.16	90.04	93.98	90.50	92.01
Average	79.21	83.08	87.12	89.60	91.87

Doi: https://doi.org/10.54216/FPA.160103
Received: July 24, 2023 Revised: November 27, 2023 Accepted: April 18, 2024

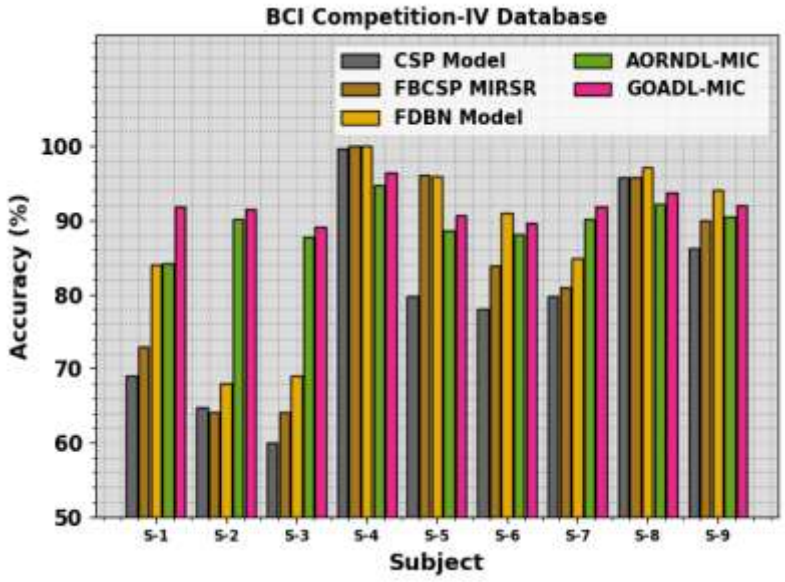

Figure 8: $Accu_y$ analysis of the GOADL-MIC system compared with other algorithms under the BCI Competition-IV dataset

Fig. 9 clarifies the average comparison analysis of the GOADL-MIC approach on the BCI Competition-IV dataset. The obtained findings display that the CSP algorithm gets poorer performance with decreased average $accu_y$ value of 79.21%. In addition, the FBCSP MIRSR system displays a closer average $accu_y$ value of 83.08%. While the FDBN and AORNDL-MIC techniques provide considerable performance, the GOADL-MIC technique emphasized a maximum average $accu_y$ of 91.87%.

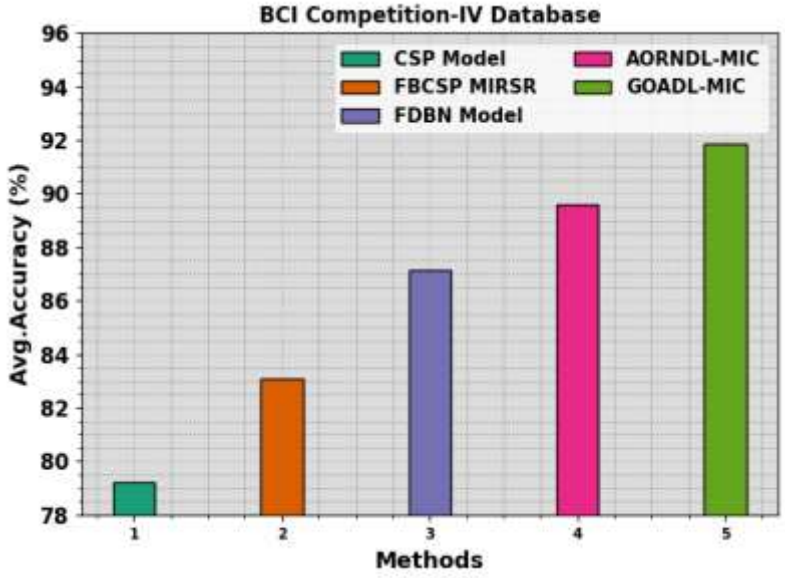

Figure 9: Average of the GOADL-MIC model under BCI Competition-IV dataset

The $accu_y$ curves for TRA and VAL shown in Fig. 10 for the GOADL-MIC algorithm with the BCI Competition-IV dataset offer esteemed insights into its efficiency in varied epochs. Predominantly, it is reliable upgrading in both TRA and TES $accu_y$ with raised epochs, representing the ability of the method in learning and recognizing patterns from the data of TRA and TES. The increased trend in TS $accu_y$ underlines the model's flexibility to the TRA dataset and capability to produce exact predictions on hidden data, highlighting skills of robust generalization.

Doi: https://doi.org/10.54216/FPA.160103
Received: July 24, 2023 Revised: November 27, 2023 Accepted: April 18, 2024

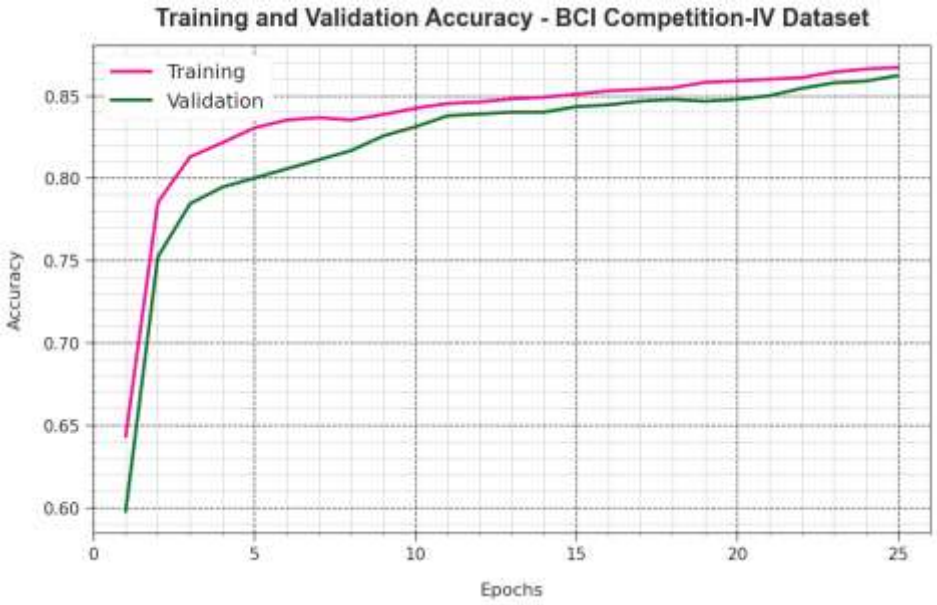

Figure 10: $Accu_y$ curve of the GOADL-MIC model with the BCI Competition-IV dataset

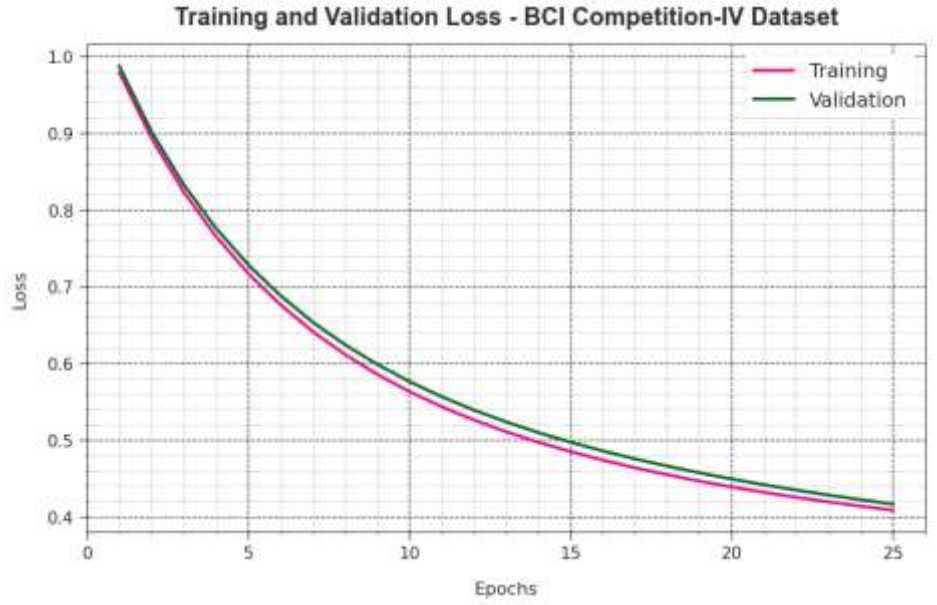

Figure 11: Loss curve of the GOADL-MIC system under BCI Competition-IV dataset

Fig. 11 exhibits an extensive summary of the TRA and TES loss values for the GOADL-MIC algorithm below the BCI Competition-IV dataset at many epochs. The TRA loss continually reduces as the method refines weights to minimalize classifier errors under both datasets. The loss curves show the model's position with the TRA data, emphasizing its ability to take patterns competently. Noteworthy is the continuous improvement of parameters in the GOADL-MIC system, intended at decreasing differences amongst predictions and actual TRA labels. Therefore, the projected model can be used for precise MI classification method.

5. Conclusion

In this work, the automated GOADL-MIC technique was introduced for the detection and classification of EEG signals for the MI classification procedure. The GOADL-MIC system comprises several processes such as pre-processing, EfficientNet-B3-based feature extraction, GOA-based hyperparameter tuning, and BiLSTM-based classification. To accomplish this, the GOADL-MIC technique initially undergoes the conversion of one dimensional-EEG signals into 2D time-frequency amplitude ones. Besides, the EfficientNet-B3 model can be applied for the effectual derivation of feature vector and its hyperparameters can be selected by using GOA.

Doi: https://doi.org/10.54216/FPA.160103
Received: July 24, 2023 Revised: November 27, 2023 Accepted: April 18, 2024

Finally, the classification of MIs takes place using the Bi-LSTM model. The experimental outcome analysis of the GOADL-MIC system is verified utilizing the BCI dataset and the results demonstrate the promising results of the GOADL-MIC method over its counter approaches in terms of different measures. Future work can focus on the design of ensemble models for the enhanced detection and classification of EEG signals

Funding: "This research received no external funding"

Conflicts of Interest: "The authors declare no conflict of interest."

References

[1] Chowdhury, R.R., Muhammad, Y. and Adeel, U., 2023. Enhancing Cross-Subject Motor Imagery Classification in EEG-Based Brain–Computer Interfaces by Using Multi-Branch CNN. Sensors, 23(18), p.7908.
[2] Zhu, H., Forenzo, D. and He, B., 2022. On the deep learning models for EEG-based brain-computer interface using motor imagery. IEEE Transactions on Neural Systems and Rehabilitation Engineering, 30, pp.2283-2291.
[3] Lee, Y.J., Lee, H.J. and Tae, K.S., 2023. Classification of EEG signals related to real and imaginary knee movements using deep learning for brain-computer interfaces. Technology and Health Care, (Preprint), pp.1-10.
[4] Mattioli, F., Porcaro, C. and Baldassarre, G., 2022. A 1D CNN for high accuracy classification and transfer learning in motor imagery EEG-based brain-computer interface. Journal of Neural Engineering, 18(6), p.066053.
[5] Jin, J., Sun, H., Daly, I., Li, S., Liu, C., Wang, X. and Cichocki, A., 2021. A novel classification framework using the graph representations of electroencephalogram for motor imagery-based brain-computer interface. IEEE Transactions on Neural Systems and Rehabilitation Engineering, 30, pp.20-29.
[6] Pham, T.D., 2023. Classification of Motor-Imagery Tasks Using a Large EEG Dataset by Fusing Classifiers Learning on Wavelet-Scattering Features. IEEE Transactions on Neural Systems and Rehabilitation Engineering, 31, pp.1097-1107.
[7] Abenna, S., Nahid, M. and Bajit, A., 2022. Motor imagery based brain-computer interface: improving the EEG classification using Delta rhythm and LightGBM algorithm. Biomedical Signal Processing and Control, 71, p.103102.
[8] Cano-Izquierdo, J.M., Ibarrola, J. and Almonacid, M., 2023. Applying deep learning in brain computer interface to classify motor imagery. Journal of Intelligent & Fuzzy Systems, (Preprint), pp.1-14.
[9] Hwaidi, J.F. and Chen, T.M., 2022. Classification of motor imagery EEG signals based on deep autoencoder and convolutional neural network approach. IEEE access, 10, pp.48071-48081.
[10] Huang, W., Chang, W., Yan, G., Yang, Z., Luo, H. and Pei, H., 2022. EEG-based motor imagery classification using convolutional neural networks with local reparameterization trick. Expert Systems with Applications, 187, p.115968.
[11] Rajalakshmi, S., AlMohimeed, I., Sikkandar, M.Y. and Begum, S.S., 2023. Optimal Deep Learning-Based Recognition Model for EEG Enabled Brain-Computer Interfaces Using Motor-Imagery. Measurement Science Review, 23(6), pp.248-253.
[12] Zhang, C., Kim, Y.K. and Eskandarian, A., 2021. EEG-inception: an accurate and robust end-to-end neural network for EEG-based motor imagery classification. Journal of Neural Engineering, 18(4), p.046014.
[13] Wang, X., Yang, R. and Huang, M., 2022. An unsupervised deep-transfer-learning-based motor imagery EEG classification scheme for brain–computer interface. Sensors, 22(6), p.2241.
[14] Zhong, X.C., Wang, Q., Liu, D., Liao, J.X., Yang, R., Duan, S., Ding, G. and Sun, J., 2023. A deep domain adaptation framework with correlation alignment for EEG-based motor imagery classification. Computers in Biology and Medicine, 163, p.107235.
[15] Cho, J.H., Jeong, J.H. and Lee, S.W., 2021. Neurograsp: Real-time eeg classification of high-level motor imagery tasks using a dual-stage deep learning framework. IEEE Transactions on Cybernetics, 52(12), pp.13279-13292.
[16] Han, Y., Wang, B., Luo, J., Li, L. and Li, X., 2022. A classification method for EEG motor imagery signals based on parallel convolutional neural network. Biomedical Signal Processing and Control, 71, p.103190.
[17] Liu, X., Xiong, S., Wang, X., Liang, T., Wang, H. and Liu, X., 2023. A compact multi-branch 1D convolutional neural network for EEG-based motor imagery classification. Biomedical Signal Processing and Control, 81, p.104456.
[18] Sun, B., Liu, Z., Wu, Z., Mu, C. and Li, T., 2022. Graph convolution neural network based end-to-end channel selection and classification for motor imagery brain-computer interfaces. IEEE transactions on industrial informatics.

Doi: https://doi.org/10.54216/FPA.160103
Received: July 24, 2023 Revised: November 27, 2023 Accepted: April 18, 2024

[19] Yahya, N., Musa, H., Ong, Z.Y. and Elamvazuthi, I., 2019. Classification of motor functions from electroencephalogram (EEG) signals based on an integrated method comprised of common spatial pattern and wavelet transform framework. Sensors, 19(22), p.4878.
[20] Abd El-Ghany, S., Elmogy, M. and El-Aziz, A.A., 2023. Computer-Aided Diagnosis System for Blood Diseases Using EfficientNet-B3 Based on a Dynamic Learning Algorithm. Diagnostics, 13(3), p.404.
[21] Ekinci, S., Izci, D. and Yilmaz, M., 2023. Efficient Speed Control for DC Motors Using Novel Gazelle Simplex Optimizer. IEEE Access.
[22] Bouazzi, Y., Yahyaoui, Z. and Hajji, M., 2024. Deep recurrent neural networks based Bayesian optimization for fault diagnosis of uncertain GCPV systems depending on outdoor condition variation. Alexandria Engineering Journal, 86, pp.335-345.
[23] S. Lemm, C. Schafer, and G. Curio, "BCI competition 2003- data set III: probabilistic modeling of sensorimotor/spl mu/ rhythms for classification of imaginary hand movements," IEEE Transactions on Biomedical Engineering, vol. 51, no. 6, pp. 1077–1080, 2004.
[24] R. Leeb, F. Lee, C. Keinrath, R. Scherer, H. Bischof, and G. Pfurtscheller, "Brain-computer communication: motivation, aim, and impact of exploring a virtual apartment," IEEE Transactions on Neural Systems and Rehabilitation Engineering, vol. 15, no. 4, pp. 473–482, 2007.
[25] Malibari, A.A., Al-Wesabi, F.N., Obayya, M., Alkhonaini, M.A., Hamza, M.A., Motwakel, A., Yaseen, I. and Zamani, A.S., 2022. Arithmetic optimization with retinanet model for motor imagery classification on brain computer interface. Journal of healthcare engineering, 2022.

Doi: https://doi.org/10.54216/FPA.160103
Received: July 24, 2023 Revised: November 27, 2023 Accepted: April 18, 2024